

## A drift model of interchange instability

E. S. Benilov and O. A. Power

Department of Mathematics, University of Limerick, Limerick, Ireland

(Received 18 December 2006; accepted 4 June 2007; published online 15 August 2007)

A set of asymptotic equations is derived, describing the dynamics of the flute mode in a magnetized plasma with cold ions, under a “local” approximation (i.e., near a particular point). The asymptotic set is then used to calculate the growth rate of interchange instability in the slab model. It is shown that, unlike the magnetohydrodynamic ordering, the drift one allows instability to occur for either sign of the pressure gradient (i.e., for both “bad” and “good” curvature of the magnetic field). It is also demonstrated that finite beta gives rise to an extra instability that does not exist in the small-beta limit. © 2007 American Institute of Physics. [DOI: 10.1063/1.2752815]

### I. INTRODUCTION

Historically, interchange (flute) instability has been mostly studied using the magnetohydrodynamic (MHD) theory (e.g., Refs. 1–3). In particular, it was shown that low-density (small-beta) tokamak plasmas are unstable if

$$\bar{p}' < -\frac{10\bar{p}}{3R}, \quad (1)$$

where  $R$  is the radius of the curvature of the magnetic field,  $\bar{p}$  is the pressure, and  $\bar{p}'$  is its derivative with respect to the distance to the tokamak’s axis (the bar implies that the corresponding quantity represents a steady state). Note that, since (1) was obtained through MHD, it is valid only for disturbances with wavelengths that are much larger than the Larmor radius ( $\lambda \gg \rho_s$ ).

Interchange instability has also been investigated using the drift ordering, which allows for  $\lambda \sim \rho_s$ . We shall note three such papers: Ref. 4 derived the dispersion relation of linear disturbances in a plasma with cold ions, Ref. 5 examined the same problem in plasmas with cold ions and small beta, and Ref. 6 studied the most general setting (arbitrary ion temperature, arbitrary beta). For the simplest case covered in all three papers (cold ions, small beta), the only example of interchange instability found involved *long-wave* disturbances, and the instability condition turned out to coincide with that of MHD;<sup>7</sup> i.e., (1).

In the present paper, we derive a set of “local” equations for drift-interchange instability of plasmas with cold ions and arbitrary beta (Sec. II) and apply it to the so-called slab model (Sec. III). The disturbance’s wavelength will not be assumed large. It will be shown that, even for a small beta, disturbances with *finite* wavelengths dramatically expand the (long-wave) instability region (1), with finite beta causing further destabilization.

### II. THE GOVERNING EQUATIONS

We shall characterize the plasma by its concentration  $n$  (quasi-neutrality implied), the respective ion and electron velocities  $\mathbf{V}_i$  and  $\mathbf{V}_e$ , the electron pressure  $p_e$  (its ion counterpart assumed negligible), and the ion mass  $m_i$  (electron inertia neglected). We shall use the following set of equations:

$$\frac{\partial n}{\partial t} + \mathbf{V}_i \cdot \nabla n + n \nabla \cdot \mathbf{V}_i = 0, \quad (2)$$

$$\frac{\nabla p_e}{n} = -e(\mathbf{E} + \mathbf{V}_e \times \mathbf{B}), \quad (3)$$

$$m_i \left( \frac{\partial \mathbf{V}_i}{\partial t} + \mathbf{V}_i \cdot \nabla \mathbf{V}_i \right) = e(\mathbf{E} + \mathbf{V}_i \times \mathbf{B}), \quad (4)$$

$$\left( \frac{\partial p_e}{\partial t} + \mathbf{V}_e \cdot \nabla p_e \right) + \frac{5p_e}{3} \nabla \cdot \mathbf{V}_e - \nabla \cdot \left[ \frac{5p_e \mathbf{B}}{3e|\mathbf{B}|^2} \times \nabla \left( \frac{p_e}{n} \right) \right] = 0, \quad (5)$$

where  $e$  is the elementary charge. The respective electric and magnetic fields  $\mathbf{E}$  and  $\mathbf{B}$  satisfy

$$\frac{\partial \mathbf{B}}{\partial t} + \nabla \times \mathbf{E} = \mathbf{0}, \quad (6)$$

$$\nabla \times \mathbf{B} = \mu_0 en(\mathbf{V}_i - \mathbf{V}_e), \quad (7)$$

$$\nabla \cdot \mathbf{B} = 0, \quad (8)$$

where  $\mu_0$  is the magnetic permeability of vacuum.

It is convenient to express  $\mathbf{V}_e$  and  $\mathbf{E}$  from (7) and (3), and substitute into Eqs. (4)–(6):

$$nm_i \left( \frac{\partial \mathbf{V}_i}{\partial t} + \mathbf{V}_i \cdot \nabla \mathbf{V}_i \right) + \nabla \cdot \left( p_e + \frac{|\mathbf{B}|^2}{2\mu_0} \right) - \frac{\mathbf{B} \cdot \nabla \mathbf{B}}{\mu_0} = \mathbf{0}, \quad (9)$$

$$\frac{\partial p_e}{\partial t} + \mathbf{V}_i \cdot \nabla p_e + \frac{5p_e}{3} \nabla \cdot \mathbf{V}_i - \frac{1}{\mu_0 en} \left( \nabla p_e - \frac{5p_e}{3n} \nabla n \right) \cdot \nabla \times \mathbf{B} - \nabla \cdot \left[ \frac{5p_e \mathbf{B}}{3e|\mathbf{B}|^2} \times \nabla \left( \frac{p_e}{n} \right) \right] = 0, \quad (10)$$

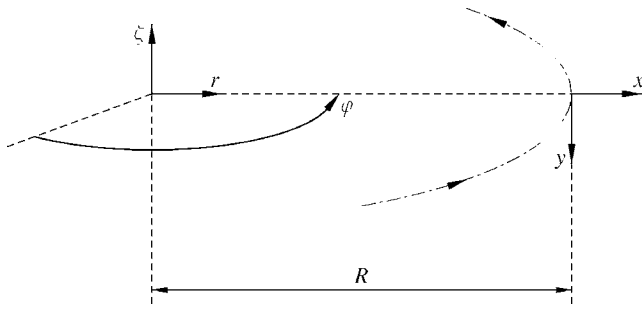


FIG. 1. The relationship between the usual cylindrical coordinates  $(r, \varphi, \zeta)$  and the modified ones  $(x, y, \varphi)$ . The latter are associated with a reference point located at a distance  $R$  from the  $\zeta$  axis ( $R^{-1}$  is, essentially, the magnetic field's curvature). The dashed-dotted curve shows the magnetic field line passing through the reference point.

$$\frac{\partial \mathbf{B}}{\partial t} + \mathbf{V}_i \cdot \nabla \mathbf{B} - \mathbf{B} \cdot \nabla V_i + \mathbf{B} \nabla \cdot \mathbf{V}_i + \frac{1}{en^2} (\nabla n) \times \nabla \left( p_e + \frac{|\mathbf{B}|^2}{2\mu_0} \right) + \nabla \times \left( \frac{1}{\mu_0 en} \mathbf{B} \cdot \nabla \mathbf{B} \right) = \mathbf{0} \quad (11)$$

[in the last equation, we have also taken into account (8)].

The curvature of the magnetic field can be conveniently described in terms of modified cylindrical coordinates  $(x, y, \varphi)$ , related to the usual cylindrical coordinates  $(r, \varphi, \zeta)$  by

$$x = r - R, \quad y = -\zeta, \quad \varphi = \varphi,$$

where  $R$  is the distance between the  $\zeta$  axis and a reference point ( $R^{-1}$  is, essentially, the magnetic field's curvature; see Fig. 1). Since we are interested in interchange (flute) instability, it is sufficient to assume two-dimensional geometry:

$$n = n(x, y, t), \quad p_e = p(x, y, t), \quad (12)$$

$$\mathbf{V}_i = u(x, y, t) \mathbf{e}_x + v(x, y, t) \mathbf{e}_y, \quad \mathbf{B} = B(x, y, t) \mathbf{e}_\varphi,$$

where  $\mathbf{e}_x$ ,  $\mathbf{e}_y$ , and  $\mathbf{e}_\varphi$  are the unit vectors directed along the corresponding axes.

We shall use the local approximation, i.e., assume that the deviations of density, pressure, and magnetic field from their respective reference values  $\bar{n}$ ,  $\bar{p}$ , and  $\bar{B}$  are small. Next, introduce the following nondimensional variables:

$$\hat{t} = \varepsilon \omega_i t, \quad (\hat{x}, \hat{y}) = \frac{(x, y)}{\rho_s}, \quad (13)$$

$$\hat{n} = \frac{n - \bar{n}}{\varepsilon \bar{n}}, \quad \hat{p} = \frac{p - \bar{p}}{\varepsilon \bar{p}}, \quad \hat{B} = \frac{B - \bar{B}}{\varepsilon \bar{B}}, \quad (\hat{u}, \hat{v}) = \frac{(u, v)}{\varepsilon \rho_s \omega_i}, \quad (14)$$

where  $\varepsilon$  is a small parameter characterizing the fields' deviations from their reference values, and

$$\rho_s = \frac{1}{e \bar{B}} \left( \frac{\bar{p} m_i}{\bar{n}} \right)^{1/2}, \quad \omega_i = \frac{e \bar{B}}{m_i}$$

are the Larmor radius and cyclotron frequency, respectively. Observe that  $\varepsilon$  makes the time scale in (13) much larger than  $\omega_i^{-1}$ ; i.e., our asymptotic derivation targets low-frequency motions.

Upon substitution of (12)–(14) into Eqs. (2) and (9)–(11), we obtain (hats omitted)

$$\varepsilon \left( \frac{\partial n}{\partial t} + u \frac{\partial n}{\partial x} + v \frac{\partial n}{\partial y} \right) + (1 + \varepsilon n) \left( \frac{\partial u}{\partial x} + \frac{\alpha u}{1 + \alpha x} + \frac{\partial v}{\partial y} \right) = 0, \quad (15)$$

$$\varepsilon (1 + \varepsilon n) \left( \frac{\partial u}{\partial t} + u \frac{\partial u}{\partial x} + v \frac{\partial u}{\partial y} \right) + \frac{\partial}{\partial x} \left( p + \frac{2B + \varepsilon B^2}{\beta} \right) + \frac{2\alpha(1 + \varepsilon B)^2}{\varepsilon \beta(1 + \alpha x)} = 0, \quad (16)$$

$$\varepsilon (1 + \varepsilon n) \left( \frac{\partial v}{\partial t} + u \frac{\partial v}{\partial x} + v \frac{\partial v}{\partial y} \right) + \frac{\partial}{\partial y} \left( p + \frac{2B + \varepsilon B^2}{\beta} \right) = 0, \quad (17)$$

$$\varepsilon^2 \left( \frac{\partial p}{\partial t} + u \frac{\partial p}{\partial x} + v \frac{\partial p}{\partial y} \right) + \frac{5\varepsilon(1 + \varepsilon p)}{3} \left( \frac{\partial u}{\partial x} + \frac{\alpha u}{1 + \alpha x} + \frac{\partial v}{\partial y} \right) - \frac{2\varepsilon^2}{\beta(1 + \varepsilon n)} \left\{ \left[ \frac{\partial p}{\partial x} - \frac{5(1 + \varepsilon p)}{3(1 + \varepsilon n)} \frac{\partial n}{\partial x} \right] \frac{\partial B}{\partial y} - \left[ \frac{\partial p}{\partial y} - \frac{5(1 + \varepsilon p)}{3(1 + \varepsilon n)} \frac{\partial n}{\partial y} \right] \right. \\ \left. \times \left[ \frac{\partial B}{\partial x} + \frac{\alpha(1 + \varepsilon B)}{\varepsilon(1 + \alpha x)} \right] \right\} + \left( \frac{\partial}{\partial x} + \frac{\alpha}{1 + \alpha x} \right) \left[ \frac{5(1 + \varepsilon p)}{3(1 + \varepsilon B)} \frac{\partial}{\partial y} \left( \frac{1 + \varepsilon p}{1 + \varepsilon n} \right) \right] - \frac{\partial}{\partial y} \left[ \frac{5(1 + \varepsilon p)}{3(1 + \varepsilon B)} \frac{\partial}{\partial x} \left( \frac{1 + \varepsilon p}{1 + \varepsilon n} \right) \right] = 0, \quad (18)$$

$$\varepsilon \left( \frac{\partial B}{\partial t} + u \frac{\partial B}{\partial x} + v \frac{\partial B}{\partial y} \right) + (1 + \varepsilon B) \left( \frac{\partial u}{\partial x} + \frac{\partial v}{\partial y} \right) + \frac{\varepsilon}{(1 + \varepsilon n)^2} \left[ \frac{\partial n}{\partial x} \frac{\partial}{\partial y} \left( p + \frac{2B + \varepsilon B^2}{\beta} \right) - \frac{\partial n}{\partial y} \frac{\partial}{\partial x} \left( p + \frac{2B + \varepsilon B^2}{\beta} \right) \right] \\ + \frac{\partial}{\partial y} \left[ \frac{2\alpha(1 + \varepsilon B)^2}{\beta \varepsilon(1 + \alpha x)(1 + \varepsilon n)} \right] = 0, \quad (19)$$

where

$$\alpha = \frac{\rho_s}{R}, \quad \beta = \frac{2\mu_0\bar{p}}{\bar{B}^2}$$

are, respectively, the nondimensional curvature of the magnetic field and the ratio of the material pressure to the magnetic one.

For tokamaks,  $\alpha$  can be safely assumed small.  $\beta$ , in turn, is small for conventional tokamaks (see Refs. 8 and 9) and order-one for spherical ones (see Refs. 9 and 10). Thus, for generality, we assume  $\beta \sim 1$ .

As a starting point of our derivation, observe that, in the limit  $\varepsilon \sim \alpha \ll 1$ , the zeroth orders of Eqs. (15), (18), and (19), all yield

$$\frac{\partial u}{\partial x} + \frac{\partial v}{\partial y} = 0. \quad (20)$$

Thus, to obtain as many asymptotic equations as we have unknowns, one generally needs to delve into higher orders—or, alternatively, combine the original equations in such a way that their zeroth orders cancel. The latter is easier in the present case, as it can be done by simply considering

$$\frac{3}{5\varepsilon(1+\varepsilon p)}(18) - \frac{1}{1+\varepsilon n}(15), \quad \frac{1}{1+\varepsilon B}(19) - \frac{1}{1+\varepsilon n}(15).$$

Keeping the leading orders only, we then obtain

$$\begin{aligned} & \frac{3}{5} \left( \frac{\partial p}{\partial t} + u \frac{\partial p}{\partial x} + v \frac{\partial p}{\partial y} \right) - \frac{\partial n}{\partial t} - u \frac{\partial n}{\partial x} - v \frac{\partial n}{\partial y} - \frac{2}{\beta} \left[ \left( \frac{3}{5} \frac{\partial p}{\partial x} - \frac{\partial n}{\partial x} \right) \frac{\partial B}{\partial y} - \left( \frac{3}{5} \frac{\partial p}{\partial y} - \frac{\partial n}{\partial y} \right) \left( \frac{\partial B}{\partial x} + \frac{\alpha}{\varepsilon} \right) \right] + \frac{\alpha}{\varepsilon} \frac{\partial(p-n)}{\partial y} \\ & + \frac{\partial(p-B)}{\partial x} \frac{\partial(p-n)}{\partial y} - \frac{\partial(p-B)}{\partial y} \frac{\partial(p-n)}{\partial x} = 0, \end{aligned} \quad (21)$$

$$\frac{\partial B}{\partial t} + u \frac{\partial B}{\partial x} + v \frac{\partial B}{\partial y} - \frac{\partial n}{\partial t} - u \frac{\partial n}{\partial x} - \frac{\alpha}{\varepsilon} u - v \frac{\partial n}{\partial y} + \frac{\partial n}{\partial x} \frac{\partial}{\partial y} \left( p + \frac{2B}{\beta} \right) - \frac{\partial n}{\partial y} \frac{\partial}{\partial x} \left( p + \frac{2B}{\beta} \right) + \frac{2\alpha}{\varepsilon\beta} \frac{\partial(2B-n)}{\partial y} = 0. \quad (22)$$

Observe also that, to zeroth order, (16) and (17) can be reduced to a single equation

$$p + \frac{2B}{\beta} + \frac{2\alpha x}{\varepsilon\beta} = \text{const} \quad (23)$$

(which implies an assumption that, at infinity, the pressure and magnetic field do not depend on  $t$ ). To recover another equation, we should bring the small terms in (16) and (17) up to the leading order, which can be achieved by deriving the vorticity equation through

$$\frac{\partial(16)}{\partial y} - \frac{\partial(17)}{\partial x}.$$

Keeping the leading order only, we then obtain

$$\begin{aligned} & \frac{\partial}{\partial y} \left( \frac{\partial u}{\partial t} + u \frac{\partial u}{\partial x} + v \frac{\partial u}{\partial y} \right) + \frac{4\alpha}{\varepsilon\beta} \frac{\partial B}{\partial y} \\ & - \frac{\partial}{\partial x} \left( \frac{\partial v}{\partial t} + u \frac{\partial v}{\partial x} + v \frac{\partial v}{\partial y} \right) = 0. \end{aligned} \quad (24)$$

The asymptotic set (20)–(24) can be simplified. Firstly, observe that (20) enables one to introduce a streamfunction  $\psi$ , such that

$$u = -\frac{\partial\psi}{\partial y}, \quad v = \frac{\partial\psi}{\partial x} \quad (25)$$

[ $\psi$  can also be interpreted as the nondimensional electric potential; thus, (25) essentially represents the  $\mathbf{E} \times \mathbf{B}$  drift]. Secondly, (23) can be used to eliminate  $B$ :

$$B = \text{const} - \frac{\alpha x}{\varepsilon} - \frac{\beta p}{2}. \quad (26)$$

Thirdly,  $\varepsilon$  has already played out its role as an indicator of small terms and can now be eliminated by setting

$$\varepsilon = 1. \quad (27)$$

Substitution of (25)–(27) into (21), (22), and (24) yields

$$\begin{aligned} & \left( \frac{\partial}{\partial t} - \frac{\partial\psi}{\partial y} \frac{\partial}{\partial x} + \frac{\partial\psi}{\partial x} \frac{\partial}{\partial y} \right) \left( \frac{3p}{5} - n \right) - \frac{\beta}{2} \left( \frac{\partial p}{\partial x} \frac{\partial n}{\partial y} - \frac{\partial p}{\partial y} \frac{\partial n}{\partial x} \right) \\ & + 2\alpha \frac{\partial(p-n)}{\partial y} = 0, \end{aligned} \quad (28)$$

$$\left( \frac{\partial}{\partial t} - \frac{\partial\psi}{\partial y} \frac{\partial}{\partial x} + \frac{\partial\psi}{\partial x} \frac{\partial}{\partial y} \right) \left( \frac{\beta p}{2} + n \right) + 2\alpha \frac{\partial(p-\psi)}{\partial y} = 0, \quad (29)$$

$$\left( \frac{\partial}{\partial t} - \frac{\partial\psi}{\partial y} \frac{\partial}{\partial x} + \frac{\partial\psi}{\partial x} \frac{\partial}{\partial y} \right) \left( \frac{\partial^2\psi}{\partial x^2} + \frac{\partial^2\psi}{\partial y^2} \right) + 2\alpha \frac{\partial p}{\partial y} = 0. \quad (30)$$

For  $\beta=0$ , set (28)–(30) is equivalent to Eqs. (6)–(8) of Ref. 5.

### III. THE SLAB MODEL

In this section, we apply (28)–(30) to the so-called slab model, where  $x$  is identified with the radial direction and  $y$ , the poloidal one. The slab geometry also implies that the tokamak's cross section is close to axial symmetry, so the steady state is independent of  $y$ .

Mathematically, the slab model corresponds to the substitution

$$n = \bar{n}'x + \tilde{n}(x, y, t), \quad p = \bar{p}'x + \tilde{p}(x, y, t), \quad \psi = \tilde{\psi}(x, y, t), \quad (31)$$

where  $\bar{n}'$  and  $\bar{p}'$  are the (steady) gradients of concentration and pressure, and the “tilded” variables describe a small disturbance superposed on the steady state. Substituting (31) into (28)–(30) and omitting nonlinear terms, we obtain

$$\begin{aligned} \frac{\partial}{\partial t} \left( \frac{3\tilde{p}}{5} - \tilde{n} \right) - \frac{\partial \tilde{\psi}}{\partial y} \left( \frac{3\bar{p}'}{5} - \bar{n}' \right) - \frac{\beta}{2} \left( \bar{p}' \frac{\partial \tilde{n}}{\partial y} - \frac{\partial \tilde{p}}{\partial y} \bar{n}' \right) \\ + 2\alpha \frac{\partial(\tilde{p} - \tilde{n})}{\partial y} = 0, \end{aligned} \quad (32)$$

$$\frac{\partial}{\partial t} \left( \frac{\beta\tilde{p}}{2} + \tilde{n} \right) - \frac{\partial \tilde{\psi}}{\partial y} \left( \frac{\beta\bar{p}'}{2} + \bar{n}' \right) + 2\alpha \frac{\partial(\tilde{p} - \tilde{\psi})}{\partial y} = 0, \quad (33)$$

$$\frac{\partial}{\partial t} \left( \frac{\partial^2 \tilde{\psi}}{\partial x^2} + \frac{\partial^2 \tilde{\psi}}{\partial y^2} \right) + 2\alpha \frac{\partial \tilde{p}}{\partial y} = 0. \quad (34)$$

We shall consider harmonic disturbances, i.e., solutions of the form

$$\begin{aligned} \tilde{n}(x, y, t) = n_0 e^{i(ky - \omega t)}, \quad \tilde{p}(x, y, t) = p_0 e^{i(ky - \omega t)}, \\ \tilde{\psi}(x, y, t) = \psi_0 e^{i(ky - \omega t)}, \end{aligned} \quad (35)$$

where  $\omega$  and  $k$  are the frequency and poloidal wavenumber of the disturbance, respectively (it can be shown that the fastest instability occurs for purely poloidal disturbances, so the  $x$ -wavenumber was assumed to be zero). Substitution of (35) into (32)–(34) yields

$$\begin{aligned} \Omega \left( \frac{3p_0}{5} - n_0 \right) + \left( \frac{3\bar{p}'}{5} - \bar{N}' \right) k \psi_0 + \frac{\beta k}{2} (\bar{p}' n_0 - \bar{N}' p_0) \\ - k(p_0 - n_0) = 0, \end{aligned} \quad (36)$$

$$\Omega \left( \frac{\beta p_0}{2} + n_0 \right) + \left( \frac{\beta \bar{p}'}{2} + \bar{N}' \right) k \psi_0 - k(p_0 - \psi_0) = 0, \quad (37)$$

$$\Omega k \psi_0 + p_0 = 0, \quad (38)$$

where

$$\Omega = \frac{\omega}{2\alpha}, \quad \bar{N}' = \frac{\bar{n}'}{2\alpha}, \quad \bar{P}' = \frac{\bar{p}'}{2\alpha}.$$

Eliminating  $n_0$ ,  $p_0$ , and  $\psi_0$  from (36)–(38), we obtain

$$\begin{aligned} \left( \frac{3}{5} + \frac{\beta}{2} \right) \Omega^3 - k \left[ 2 + \left( 1 + \bar{N}' + \frac{\beta \bar{P}'}{2} \right) \frac{\beta}{2} \right] \Omega^2 \\ - \left[ 1 + \left( \frac{3}{5} + \frac{\beta}{2} \right) \bar{P}' - k^2 \left( 1 + \frac{\beta \bar{P}'}{2} \right) \right] \Omega \\ + k \left( 1 + \frac{\beta \bar{P}'}{2} \right) \left( 1 + \bar{N}' + \frac{\beta \bar{P}'}{2} \right) = 0. \end{aligned} \quad (39)$$

This equation (dispersion relation) determines  $\Omega$  and, thus, the stability properties of the flute mode: if, for some  $k$ , there are solutions with  $\text{Im } \Omega > 0$ , the plasma is unstable.

#### A. The MHD limit

The MHD ordering corresponds to the long-wave limit and the assumption  $\Omega = O(1)$  as  $k \rightarrow 0$ . Applying these to (39), we obtain

$$\left( \frac{3}{5} + \frac{\beta}{2} \right) \Omega^2 - \left[ 1 + \left( \frac{3}{5} + \frac{\beta}{2} \right) \bar{P}' \right] = 0.$$

One can see that instability occurs when

$$\bar{P}' < -\frac{1}{\frac{3}{5} + \frac{\beta}{2}}, \quad (40)$$

which is the nondimensional equivalent of the classical result of Refs. 1 and 2.

#### B. The case of small beta

For  $\beta=0$ , Eq. (39) has been examined in the long-wave limit in Ref. 5. It was shown that instability occurs if

$$\bar{P}' < -\frac{5}{3}, \quad (41)$$

which is the small- $\beta$  equivalent of (40) [and the nondimensional equivalent of (1)]. It turns out, however, that there are cases where long-wave disturbances are stable, but instability still occurs at medium wavelengths ( $k \sim 1$ ).

In order to consider arbitrary  $k$ , rewrite (39) <sub>$\beta=0$</sub>  in the form

$$\frac{3\kappa}{5} C^3 - 2\kappa C^2 - \left( 1 + \frac{3\bar{P}'}{5} - \kappa \right) C + \bar{N}' + 1 = 0, \quad (42)$$

where

$$C = \frac{\Omega}{k}, \quad \kappa = k^2. \quad (43)$$

The main characteristics of any instability are the marginally stable wavenumbers; i.e., the values of  $k$  separating stable and unstable regions in the  $k$ -space. In what follows, we shall develop a tool for finding them.

Equation (42), just like any other cubic equation, can be represented in the form

$$[(C - a)^2 + b](C - d) = 0,$$

where  $a$ ,  $b$ , and  $d$  are real functions of  $\kappa$  (and also of  $\bar{P}'$ ,  $\bar{N}'$ ). The potentially unstable solution is, then,

$$C = a(\kappa) + \sqrt{b(\kappa)}. \tag{44}$$

Observe that, for a marginally stable (MS) value  $\kappa_{MS}$ ,  $b(\kappa)$  must change sign; hence, its Taylor expansion is, generally,

$$b \rightarrow \left(\frac{db}{d\kappa}\right)_{\kappa=\kappa_{MS}} (\kappa - \kappa_{MS}) + \frac{1}{2} \left(\frac{d^2b}{d\kappa^2}\right)_{\kappa=\kappa_{MS}} (\kappa - \kappa_{MS})^2 + \dots \text{ as } \kappa \rightarrow \kappa_{MS}. \tag{45}$$

Note that (44) and (45) imply

$$\frac{dC}{d\kappa} \rightarrow \infty \text{ as } \kappa \rightarrow \kappa_{MS}.$$

This condition can be used as a means of locating the MS values of  $\kappa$  and, eventually, the MS values of  $\bar{P}'$  and  $\bar{N}'$ .

Indeed, differentiating the dispersion relation (42) with respect to  $\kappa$ , one can obtain

$$\frac{dC}{d\kappa} = \frac{-\frac{3}{5}C^3 + 2C^2 - C}{\frac{9\kappa}{5}C^2 - 4\kappa C - 1 - \frac{3}{5}\bar{P}' + \kappa}. \tag{46}$$

Hence,  $C$  may have infinite derivative only if

$$\frac{9\kappa}{5}C^2 - 4\kappa C - 1 - \frac{3}{5}\bar{P}' + \kappa = 0. \tag{47}$$

Next, consider a pair of MS values,  $(\kappa_{MS1}, \kappa_{MS2})$ , describing an instability interval in the  $\kappa$  axis. When  $\bar{P}'$  and  $\bar{N}'$  approach their MS values, the instability interval shrinks and vanishes; i.e.,  $\kappa_{MS1}$  and  $\kappa_{MS2}$  merge and disappear. Hence,  $dC/d\kappa$  must become regular, which is possible only if the numerator of (46) vanishes at the same point where the denominator does, which yields

$$-\frac{3}{5}C^3 + 2C^2 - C = 0. \tag{48}$$

Finally, the definition of  $\kappa$  [see (43)] implies

$$\kappa \geq 0. \tag{49}$$

Now, eliminating  $\kappa$  and  $C$  from (42) and (47)–(49) one can obtain the following curves on the  $(\bar{P}', \bar{N}')$  plane:

$$1 + \bar{N}' = 0, \quad 1 + \frac{3\bar{P}'}{5} \geq 0, \tag{50}$$

$$1 + \bar{N}' = \frac{5 + \sqrt{10}}{3} \left(1 + \frac{3\bar{P}'}{5}\right), \quad 1 + \frac{3\bar{P}'}{5} \geq 0, \tag{51}$$

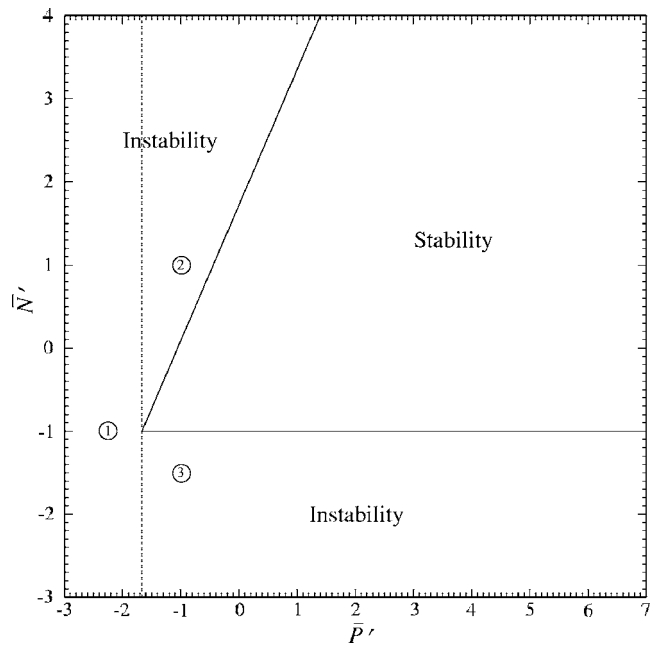


FIG. 2. The marginal stability curve on the  $(\bar{P}', \bar{N}')$  plane, for  $\beta=0$ . The nondimensional gradients  $\bar{P}'$ ,  $\bar{N}'$  of the pressure and concentration are given by (56). The parameter values to the left from the dotted line are unstable in the long-wave limit. The dispersion curves corresponding to the “numbered” point are shown in Fig. 3.

$$1 + \bar{N}' = \frac{5 - \sqrt{10}}{3} \left(1 + \frac{3\bar{P}'}{5}\right), \quad 1 + \frac{3\bar{P}'}{5} \leq 0. \tag{52}$$

One should keep in mind, however, that some of these solutions correspond to vanishing of one of several instability regions and, thus, are not MS curves. To eliminate these, we carried out “numerical sampling”; i.e., computed  $C(\kappa)$  from

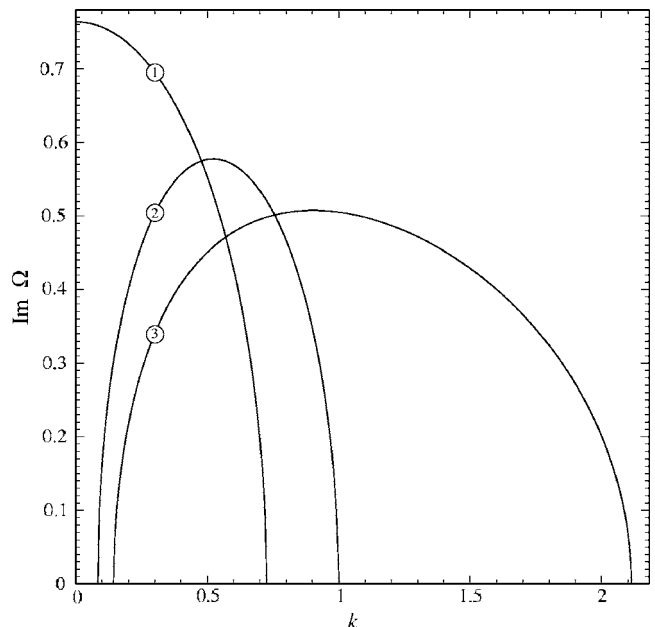


FIG. 3. The growth rate  $\text{Im } \Omega$  vs the poloidal wavenumber  $k$ , for  $\beta=0$ . The numbers of curves correspond to the numbers of the points marked in Fig. 2. Observe that curve 1 is the only one with long-wave ( $k \rightarrow 0$ ) instability.

(42) for particular points on both sides of curves (50)–(52). It turned out that (52) is *not* a MS curve, as it separates cases with one instability region and those with two. Sampling also helped us to determine which sides of the MS curves (50) and (51) correspond to instability, and the results are shown in Fig. 2.

Note also that, in addition to a merger of two MS  $\kappa$ -values, stabilization may occur if the instability region “exits” through the zero or infinity. To detect such cases, (42) was examined as  $\kappa \rightarrow 0$  and  $\kappa \rightarrow \infty$ . The former limit yields  $\bar{P}' = -5/3$ , but sampling shows that this condition separates cases where the instability interval is adjacent to, or detached from, zero (see Fig. 3; this figure also illustrates the fact that, for MS values of  $k$ ,  $dC/dk = \infty$ ). Finally, it can be readily shown that (42) has no unstable solutions as  $\kappa \rightarrow \infty$ .

Thus, the instability region on the  $(\bar{P}', \bar{N}')$  plane is

$$\begin{aligned} \bar{P}' &< -\frac{5}{3 + \frac{5\beta}{2}}, \\ \text{or } \bar{P}' &> -\frac{5}{3 + \frac{5\beta}{2}}, \quad \bar{N}' < -1 - \frac{\beta\bar{P}'}{2}, \\ \text{or } \bar{P}' &> -\frac{5}{3 + \frac{5\beta}{2}}, \quad \bar{N}' > -1 - \frac{\beta\bar{P}'}{2} + \frac{5 + \sqrt{10}}{3} \left( 1 + \frac{3\bar{P}'}{5} + \frac{\beta\bar{P}'}{2} \right), \end{aligned} \tag{54}$$

which is similar to its zero- $\beta$  counterpart (53). It turns out, however, that finite  $\beta$  can destabilize *large* wavenumbers.

Indeed, assuming  $\Omega = O(k)$  as  $k \rightarrow \infty$ , one can reduce Eq. (39) to

$$\begin{aligned} \left( \frac{3}{5} + \frac{\beta}{2} \right) \Omega^2 - k \left[ 2 + \left( 1 + \bar{N}' + \frac{\beta\bar{P}'}{2} \right) \frac{\beta}{2} \right] \Omega \\ + k^2 \left( 1 + \frac{\beta\bar{P}'}{2} \right) = 0 \quad \text{as } k \rightarrow \infty. \end{aligned} \tag{55}$$

Hence, the plasma is unstable if

$$\left[ 2 + \left( 1 + \bar{N}' + \frac{\beta\bar{P}'}{2} \right) \frac{\beta}{2} \right]^2 < 4 \left( \frac{3}{5} + \frac{\beta}{2} \right) \left( 1 + \frac{\beta\bar{P}'}{2} \right). \tag{56}$$

As a result, the instability region on the  $(\bar{P}', \bar{N}')$  plane noticeably expands, especially for positive  $\bar{P}'$  (see Fig. 4).

Furthermore, since (55) and (56) imply that  $\text{Im } \Omega \rightarrow \infty$  as  $k \rightarrow \infty$ , the new instability causes an “ultraviolet catastrophe”; i.e., mathematically, disturbances explode (develop singularity) in a finite time. Physically, this effect ought to be restricted by dissipation (not included in the present work).

$$\begin{aligned} \bar{P}' &< -\frac{5}{3}, \\ \text{or } \bar{P}' &> -\frac{5}{3}, \quad \bar{N}' < -1, \\ \text{or } \bar{P}' &> -\frac{5}{3}, \quad \bar{N}' > -1 + \frac{5 + \sqrt{10}}{3} \left( 1 + \frac{3\bar{P}'}{5} \right), \end{aligned} \tag{53}$$

which is considerably wider than what is predicted by the long-wave condition (41) (see Fig. 2). Interestingly, instability can even occur if the pressure gradient is positive (i.e., the magnetic field’s curvature is “good”).

### C. The case of finite beta

For  $\beta \neq 0$ , the instability condition involving small/medium MS wavenumbers is

Still, one can qualitatively conclude that finite  $\beta$  is a strong destabilizing influence, which is also confirmed by Fig. 5.

To put the instability conditions (54), (56) in a physical context, we relate the nondimensional gradients  $\bar{P}'$ ,  $\bar{N}'$  to their dimensional counterparts,  $\bar{p}'$ ,  $\bar{n}'$ :

$$\bar{P}' = \frac{R\bar{p}'}{2\bar{p}}, \quad \bar{N}' = \frac{R\bar{n}'}{2\bar{n}}, \tag{57}$$

where  $\bar{p}$  and  $\bar{n}$  are the dimensional pressure and concentration, respectively, and  $R$  is the radius of the magnetic field’s curvature. Now, estimating  $\bar{p}' \sim \bar{p}/r$  and  $\bar{n}' \sim \bar{n}/r$ , where  $r$  is the minor radius of the tokamak, one can see that  $\bar{P}'$  and  $\bar{N}'$  range from zero to values comparable to the tokamak’s aspect ratio.

### IV. COMPARISON WITH PREVIOUS WORK

In order to understand why the full extent of drift-interchange instability has not been spotted earlier, note that it was examined mainly for long-wave disturbances,<sup>5,6</sup> which are considerably less unstable. There was also a lot of work

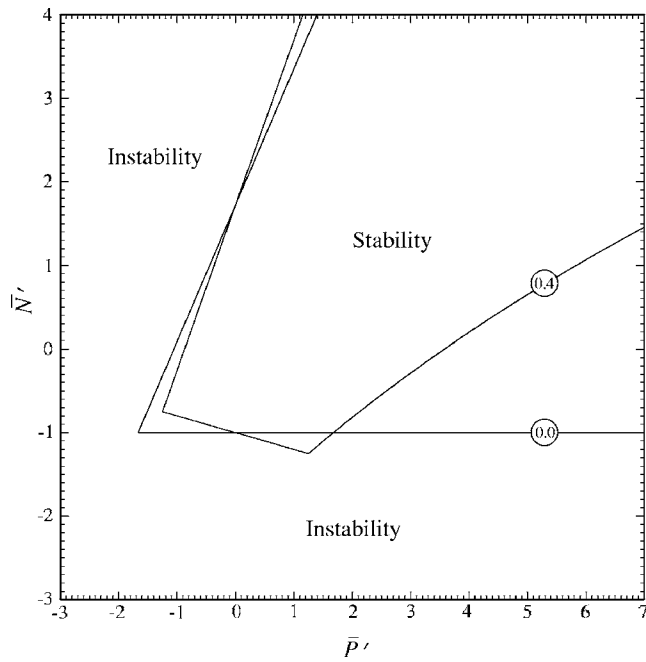


FIG. 4. Marginal stability curves on the  $(\bar{P}', \bar{N}')$  plane. The nondimensional gradients  $\bar{P}'$ ,  $\bar{N}'$  of the pressure and concentration are given by (56). The curves are marked with the corresponding values of  $\beta$ .

(e.g., Refs. 1–3) under the MHD ordering—which, however, does not describe short ( $\sim \rho_s$ ) wavelengths where “our” instability takes place.

Finally, Ref. 4 dealt with a model similar to ours, under an additional assumption of large aspect ratio,

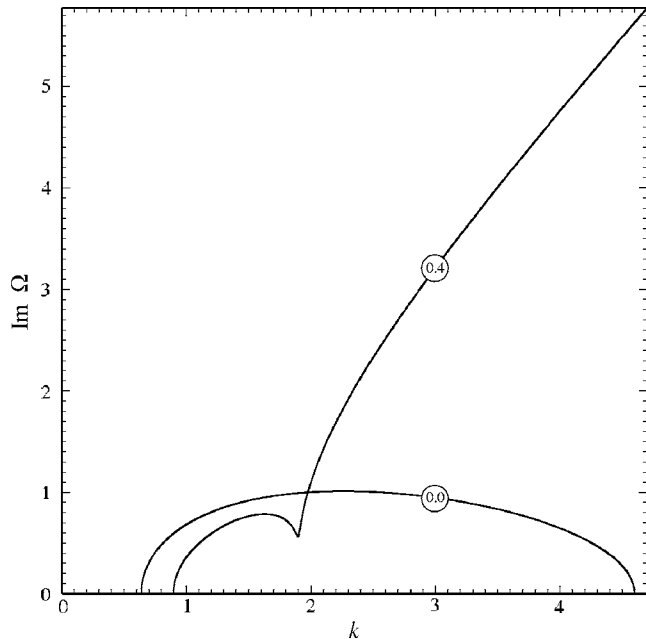


FIG. 5. The growth rate  $\text{Im } \Omega$  vs the poloidal wavenumber  $k$ , for  $\bar{P}'=4$ ,  $\bar{N}'=-3$ . The curves are marked with the corresponding values of  $\beta$ . Note that, for  $\beta=0.4$ , the instability region stretches to infinity ( $k \rightarrow \infty$ ).

$$\frac{r}{R} \ll 1. \quad (58)$$

Unlike this work, however, Ref. 4 did *not* require

$$\frac{\rho_s^2}{rR} \ll 1 \quad (59)$$

[which condition is implied by our ordering, (12)–(14)]. Accordingly, the (58) limit of our dispersion relation (39) coincides with the (59) limit of Eq. (54) of Ref. 4. The two relations, however, were examined differently: we examined ours in the general form and found instabilities, whereas Hassam and Lee<sup>4</sup> investigated theirs for certain limits, none of which happened to be unstable (except for the long-wave limit and a relatively narrow range  $\beta \sim r/R \ll 1$ ,  $\bar{N}'/\bar{P}' \ll 1$ ).

Finally, Ref. 4 found a low-frequency instability, given by their formula (52). To understand why this instability is not present in our analysis, observe that an *a posteriori* check of (52) for compliance with the underlying assumption (that the frequency is indeed low) requires  $\rho_s^2/rR \gg 1$ , which is the opposite to condition (59) implied in the present paper.

## V. SUMMARY AND CONCLUDING REMARKS

Thus, we have derived asymptotic set (28)–(30) describing drift-interchange instability of magnetized plasma with cold ions, under a “local” approximation (i.e., near a particular point). Using the set, we obtained instability criteria (54), (56). It turned out that, even for a small beta, instability may occur for either sign of the pressure gradient (i.e., for both “bad” and “good” curvatures of the magnetic field). Finite beta, in turn, gives rise to an extra instability [described by (56)]. This new instability is particularly strong, as, spectrally, it stretches to infinitely short waves and, thus, can cause an ultraviolet catastrophe.

Finally, note that we have used the asymptotic set (28)–(30) only to examine linear stability, but it can also be employed for modeling nonlinear phenomena, such as turbulence, transport barriers, etc.

<sup>1</sup>M. N. Rosenbluth and C. L. Longmire, *Ann. Phys.* **1**, 120 (1957).

<sup>2</sup>I. B. Bernstein, E. A. Frieman, M. D. Kruskal, and R. M. Karlsruh, *Proc. R. Soc. London, Ser. A* **244**, 17 (1958).

<sup>3</sup>J. M. Green and J. L. Johnson, *Plasma Phys.* **10**, 729 (1968).

<sup>4</sup>A. B. Hassam and Y. C. Lee, *Phys. Fluids* **27**, 438 (1984).

<sup>5</sup>V. Naulin, J. Nycander, and J. J. Rasmussen, *Phys. Rev. Lett.* **81**, 4148 (1998).

<sup>6</sup>J. Kesner, *Phys. Plasmas* **7**, 3837 (2000).

<sup>7</sup>In addition to the MHD instability, Ref. 4 also found an instability in the limit  $\rho_s^2/rR \gg 1$ , where  $r \sim \bar{p}/\bar{p}'$  is the spatial scale of the pressure field variability (in most cases,  $r$  is of the order of the tokamak’s minor radius). This issue is elaborated in Sec. IV.

<sup>8</sup>D. Boucher, J. W. Connor, W. A. Houlberg *et al.*, *Nucl. Fusion* **40**, 1955 (2000).

<sup>9</sup>Y.-K. M. Peng, P. J. Fogarty, and T. W. Burgess, *IEEJ Trans. Fund. Mat.* **125-A**, 857 (2005).

<sup>10</sup>E. J. Synakowski, M. G. Bell, R. E. Bell *et al.*, *Nucl. Fusion* **43**, 1653 (2003).